buildings

MDPI

Article

Modeling the Impact of Building-Level Flood Mitigation Measures Made Possible by Early Flood Warnings on Community-Level Flood Loss Reduction

Omar M. Nofal [1], John W. van de Lindt [1,*], Harvey Cutler [2], Martin Shields [2] and Kevin Crofton [2]

[1] Department of Civil and Environmental Engineering, Colorado State University, Fort Collins, CO 80523, USA; omar.nofal@colostate.edu
[2] Department of Economics, Colorado State University, Fort Collins, CO 80523, USA; harvey.cutler@colostate.edu (H.C.); martin.shields@colostate.edu (M.S.); Kevin.crofton@colostate.edu (K.C.)
* Correspondence: jwv@engr.colostate.edu; Tel.: +1-970-491-6697

Abstract: The growing number of flood disasters worldwide and the subsequent catastrophic consequences of these events have revealed the flood vulnerability of communities. Flood impact predictions are essential for better flood risk management which can result in an improvement of flood preparedness for vulnerable communities. Early flood warnings can provide households and business owners additional time to save certain possessions or products in their buildings. This can be accomplished by elevating some of the water-sensitive components (e.g., appliances, furniture, electronics, etc.) or installing a temporary flood barrier. Although many qualitative and quantitative flood risk models have been developed and highlighted in the literature, the resolution used in these models does not allow a detailed analysis of flood mitigation at the building- and community level. Therefore, in this article, a high-fidelity flood risk model was used to provide a linkage between the outputs from a high-resolution flood hazard model integrated with a component-based probabilistic flood vulnerability model to account for the damage for each building within the community. The developed model allowed to investigate the benefits of using a precipitation forecast system that allows a lead time for the community to protect its assets and thereby decreasing the amount of flood-induced losses.

Keywords: flood fragility analysis; flood loss analysis; flood damage analysis; flood risk analysis

Citation: Nofal, O.M.; van de Lindt, J.W.; Cutler, H.; Shields, M.; Crofton, K. Modeling the Impact of Building-Level Flood Mitigation Measures Made Possible by Early Flood Warnings on Community-Level Flood Loss Reduction. *Buildings* **2021**, *11*, 475. https://doi.org/10.3390/buildings11100475

Academic Editor: Enrico Tubaldi

Received: 27 August 2021
Accepted: 11 October 2021
Published: 14 October 2021

1. Introduction

Flood hazards cause severe damage to buildings and infrastructure around the world with an annual loss bill in terms of billions of dollars. The severity and frequency of these events have increased substantially worldwide over the last decade [1]. The subsequent economic losses resulting from these events have revealed the vulnerability of the impacted communities [2–5]. The current flood risk literature focuses on modeling the direct and indirect economic flood losses to the built environment [6–9]. The focus also includes reducing the amount of flood losses using nature-based mitigation interventions using novel concepts such as "Sponge Cities, and sustainable urban drainage systems" [10]. Most of the flood risk mitigation strategies are centralized on hazard control measures (e.g., levees) with less focus on flood exposure and vulnerability mitigation and adaptation measures. Although these studies substantially contribute to the growing literature of flood risk and mitigation analysis, the modeling resolution used in these studies does not enable detailed flood mitigation analysis at the building- and community level. The fidelity of the engineering models used to predict the amount of flood losses mainly depends on the resolution used to model the flood risk components including hazard, exposure, and vulnerability. There is a debate in the literature on the level of details needed for a flood risk analysis that allows risk-informed decisions [11] and how sensitive the flood damage

estimation is to the different analysis resolutions [12]. The methods that have been used to estimate flood risk were reviewed by several researchers over the years [13–18] which revealed that flood-related data scarcity along with the ability to propagate uncertainties in the flood damage models are the most challenging to develop fully probabilistic flood risk models. Table 1 shows a list of the used abbreviation within this paper.

Table 1. Acronym description.

Acronym	Description
DEM	Digital elevation map
FEMA	Federal emergency management agency
HAZUS-MH	Hazards United States multi-hazard
AQPI	Advanced quantitative precipitation information
NOAA	National oceanic and atmospheric administration
NWP	Numerical weather prediction
DS	Damage state
BIM	Building information model
GIS	Geographical information system
IM	Intensity measure
Lf	Total building fragility-based losses in monetary term
Bldg_DS	Building damage state
Lrci	Cumulative replacement cost ratio corresponding to DSi
Vt	Total building cost (replacement cost)
P_in_DS	Probability of being in a damage state
FFE	First-floor elevation
μ	Mean component resistance
σ	Standard deviation of the component resistance
GDP	Gross domestic product
GE	Ground elevation
WSE	Water surface elevation

Flood risk modeling requires detailed flood hazard mapping to identify the flood extent and the spatial variation in the flood inundation across the community. Flood hazard models are usually based on detailed hydrologic and hydrodynamic analysis which use rainfall, land use, soil type, and digital elevation map (DEM) to account for the flood hazard characteristics (e.g., depth, velocity, duration, etc.) [19]. The analysis resolution is highly dependent on the quality of data which affects all downstream analyses. For example, low-resolution land-use maps could result in misleading water surface runoff and subsequently non-accurate flood hazard maps. Therefore, Landsat-8 images can be used to develop land-use maps and detect the temporal changes in land-cover [20]. The different resolution and complexities of flood hazard modeling approaches were also reviewed in a series of papers [21–23] which confirmed that 2D flood hazard models are considered sufficient to capture reliable flood hazard characteristics for flood risk analysis [24]. For flood exposure, the availability of data related to people and physical systems controls the exposure analysis resolution. For example, flood exposure analysis can be carried out at a coarse resolution such as the land-use-, census tract-, and census block-level [25–27] or at a fine resolution such as parcel and building-level [28–31]. For flood vulnerability, there are a number of analysis resolutions that have been used in the literature ranging from land-use level [27] to building level [32,33] and component level [34–36]. Currently, flood-depth damage functions are considered the most common and accepted type of flood vulnerability functions [28]. These functions are based on empirical data collected from either damage surveys, field studies, phone surveys, or reported insurance losses.

Multiple building-level flood loss assessments for communities were performed using different types of damage functions and different digital elevation map resolutions (DEM) [37]. Additionally, a climate-adjusted flood risk model at the single property level was developed by the First-Street Foundation to introduce an open-source economic-focused flood risk analysis tool [38]. The Federal Emergency Management Agency (FEMA)

developed HAZUS-MH in the early 1990s which is now considered the major risk analysis tool that has been used widely in the U.S for multiple natural hazards. The HAZUS-MH flood model mainly depends on flood-depth damage functions for a suite of building occupancies that represents the multiple sectors within a community [39]. However, the flood-depth damage function does not allow propagating the uncertainties associated with the damage evaluation process since the amount of flood damage is qualitatively estimated from the outside of buildings based on visual observations [40,41]. Recently, the concept of flood fragility functions was developed which included empirical [42] and numerical [33,34] approaches that allow uncertainty propagation across the damage modeling process. The ability to calculate probabilistic flood damage using fragility functions can then provide the necessary input for risk-informed decision support. Nofal and van de Lindt developed a portfolio of 15 building archetypes to enable community-level probabilistic flood vulnerability analysis [43] by using a component-based approach to develop flood fragility functions for each building within the portfolio. That methodology allowed detailed flood mitigation analysis at the component-, building-, and community level [44–47]. That methodology can also enable a quantitative building-level flood mitigation analysis that quantifies the impact of early flood warnings on the amount of flood losses.

The current advances in hydro-meteorological observations in terms of precipitation monitoring and rainfall forecasting can allow more efficient water resource management and better flood mitigation and evacuation planning [48,49]. These advantages are, in turn, reflected in the direct and indirect flood economic losses [50]. Recently, an advanced quantitative precipitation information (AQPI) system was developed by the National Oceanic and Atmospheric Administration (NOAA) to provide 6 to perhaps 8 h of lead time before incoming rainfall storms. The AQPI system consists of advanced radar weather sensors, data assimilation, numerical weather prediction (NWP) and hydrological models, and system integration to support weather and flood forecasting and warnings dissemination which was fully introduced by Johnson et al. [51]. With more than 6 h of early flood warnings, households may be able to move vehicles to a higher elevation, elevate water-sensitive components, and in some cases set up a temporary flood barrier system. Although Johnson et al., provided detailed insight about the regional benefits of the AQPI system using general indicators [51], the analysis is still not detailed enough to capture all the advantages of the advanced flood warnings provided by the AQPI system. Therefore, high-resolution physics-based loss models (e.g., flood risk analysis) can be used to capture the potential impact of these advances.

The state of the current literature necessitates developing an approach that allows quantifying the impact of using early flood warning systems on the total economic flood loss reduction. This approach should account for the possible building- and component-level mitigation intervention within the lead time provided by the early flood warning system. This should be done using a quantitative model that allows propagating uncertainties in the flood damage assessment process. Therefore, in this paper, a novel high-resolution flood risk model was developed to quantify the impact of early flood warning using the AQPI system on the amount of flood loss reduction at the building- and community level. The developed approach uses component-based flood fragility functions to account for the amount of damage/loss corresponding to each building within the community. Then, the impact of using specified building-level flood mitigation measures that can be completed within six to ten hours of the flood warning lead time on the direct flood losses was calculated. High-resolution flood hazard, exposure, and vulnerability models were developed to be used as inputs for the developed flood damage/loss model. A 2D hydrodynamic approach was applied to model the flood inundation across the community. The community was modeled using detailed information for building occupancy, foundation type, number of stories, and construction material. A mapping algorithm was developed to map the portfolio of 15 building archetypes across the community using the building information data. The flood inundation model was then overlaid with the community model to identify the flood hazard intensity at each building. A specific fragility function corresponding

to each building archetype was then used to account for the probability of being in each damage state (DS) and its corresponding loss ratio. Then, a set of building-level flood mitigation measures were modeled with updated vulnerability functions which included, for example, elevating water-sensitive components and using flood barriers. Different scenarios for these mitigation measures were investigated as well and their corresponding amount of flood loss reduction has been quantified. The significance of the developed model was confirmed after investigating the impact of early flood warnings using the AQPI system on the amount of flood loss reduction using Santa Clara County, California, as an example community.

2. Methodology

2.1. Advanced Quantitative Precipitation Information System (AQPI)

The AQPI system consists of a set of radar weather sensors along with weather prediction numerical models, data assimilation platforms, and hydrologic models to provide an integrated system that can support weather and flood forecasting. Such a system provides an improved spatio-temporal prediction of severe storms with proper tracking and prediction of rainfall events [51]. The AQPI system is being used in the San Francisco (SF) Bay Area to enhance weather forecasting and provide lead time before severe rainfall events. Figure 1 shows the coverage of X-band radars over SF. This system is expected to provide a 6 to 8 h lead time of incoming severe rainfall storms which is crucial for mitigation and evacuation planning. More details about the AQPI system and its essential benefits can be found in a recent paper [51].

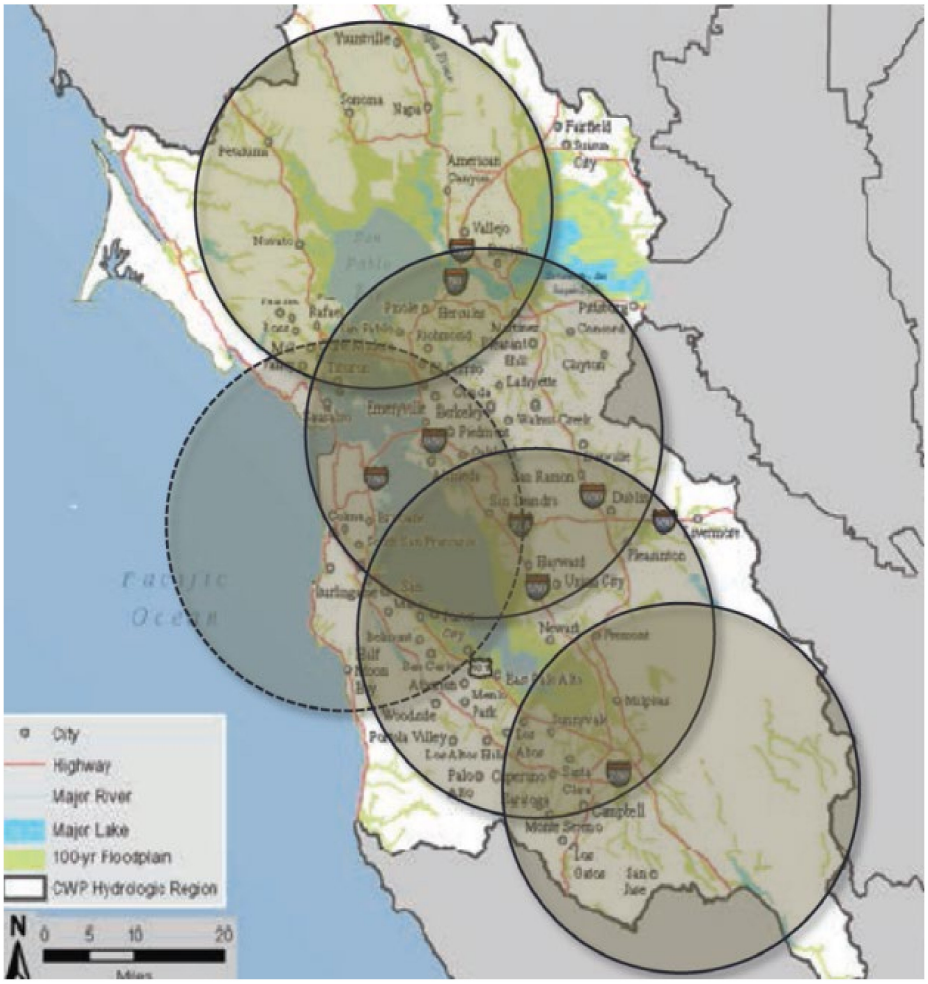

Figure 1. The coverage of the X-band radar system over the San Francisco Bay Area, CA, USA.

2.2. Community Modeling

Community modeling requires detailed information about the buildings within this community which was accomplished using a combined BIM-GIS model to develop a high-resolution model of a community. The BIM model was used to identify the different building components for a portfolio of building archetypes and then the flood susceptibility of these components was used to account for the flood vulnerability of the entire building. A portfolio of 15 flood archetypes developed by Nofal and van de Lindt [43] was used to model the flood vulnerability of each building. These vulnerability functions were validated with the HAZUS stage-damage functions which were fully illustrated herein [43]. This portfolio includes a number of building occupancies with different building characteristics which are believed to be sufficient enough to populate the building stock within a community. A very brief description of each building archetype is provided in Table 2 and more details are available in a recent study [43]. A GIS model was used to identify the different building occupancies along with other physical characteristics needed to model the physical flood vulnerability of the whole community. This was carried out by using detailed parcel information retrieved from tax assessor data [52] which includes an array of information for the buildings within each parcel including building use, age, value, number of stories, construction material, foundation type, among other building information. Although this data provides more than 400 building occupancies, the building archetype portfolio only includes 15 building archetypes. Therefore, a mapping algorithm was developed to map the 15 building archetypes to each building within the community using the tax assessor data. The conditions used for the mapping algorithm mainly depend on the building's standardized use, construction material, number of stories, foundation type, and building footprint area. Figure 2 shows a schematic representation of how the 15-building archetype portfolio was mapped to an example community.

Table 2. Flood building archetypes description [43].

Archetype	Building Description
F1	One-story residential building on a crawlspace foundation
F2	One-story residential building on a slab-on-grade foundation
F3	Two-story residential building on a crawlspace foundation
F4	Two-story residential building on a slab-on-grade foundation
F5	Small grocery store/Gas station with a convenience store (Small business)
F6	Super retail building (strip mall)
F7	Small multi-business building
F8	Super shopping center
F9	Industrial building
F10	One-story School
F11	Two-story School
F12	Hospital
F13	Community center (church)
F14	Office building
F15	Warehouse (small/large box)

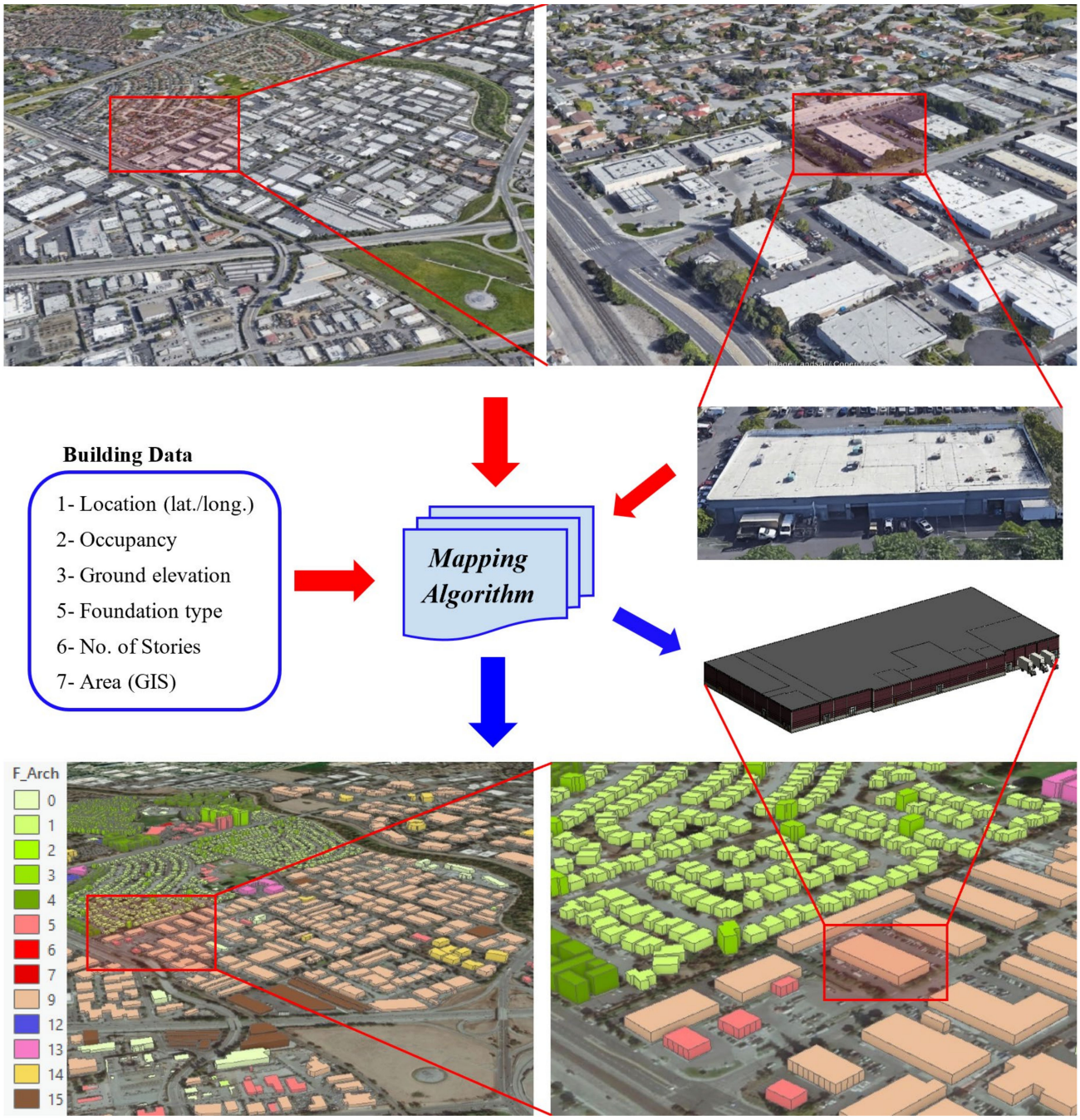

Figure 2. A schematic representation shows how a portfolio of building archetypes are mapped to buildings within a community based on detailed building data.

2.3. Flood Risk Analysis

A high-resolution probabilistic flood risk analysis methodology was used to provide a linkage between the output from a 2D flood hazard simulation and a component-based probabilistic flood vulnerability function. Figure 3 shows a schematic flow chart for this framework depicting the main steps for each analysis stage. The framework includes developing a hydrologic model using detailed soil and land use information along with detailed precipitation data to account for the flow discharge in the main streams. Then, a hydrodynamic model was developed to account for the spatial distribution of the flood hazard inundation across the community including flood depth and flood duration. The exposure model of the community was developed using the building information provided

by tax assessor data as described earlier. Afterwards, the value of the flood hazard intensity (flood depth) at each building was calculated and a building archetype was mapped based on the building characteristics. The exceedance probability of each damage state (DS) for each building was then calculated by interpolating the fragility curves/surfaces at the value of the hazard intensity [$P\ (DS_i \mid IM = x)$]. For flood loss analysis, the probability of being in each DS was calculated and a DS was assigned to each building based on the maximum probability of being in each DS using Equation (1). Then, the flood losses as a percentage of the building market were calculated by multiplying the probability of being in each DS by the replacement cost of each DS using Equation (2) which has been fully illustrated herein [43].

$$Bldg\_DS(IM = x) = \underset{i=0}{\overset{i=4}{Max}}(DS_i) \rightarrow [P(DS_i|IM = x) - P(DS_{i+1}|IM = x)] \quad (1)$$

$$L_f(IM = x) = \sum_{i=0}^{4}[P(DS_i|IM = x) - P(DS_{i+1}|IM = x)] \times Lr_{ci} \times V_t \quad (2)$$

where $Bldg\_DS\ (IM = x)$ is the building assigned DS at $IM = x$, $L_f\ (IM = x)$ = total building fragility-based losses in monetary terms at $IM = x$ (replacement or repair cost), $P\ (DS_i \mid IM = x)$ = exceedance probability of DS_i at $IM = x$, $P\ (DS_{i+1})$ = exceedance probability of DS_{i+1} at $IM = x$, Lr_{ci} = cumulative replacement cost ratio corresponding to DS_i, and V_t = total building cost (replacement cost).

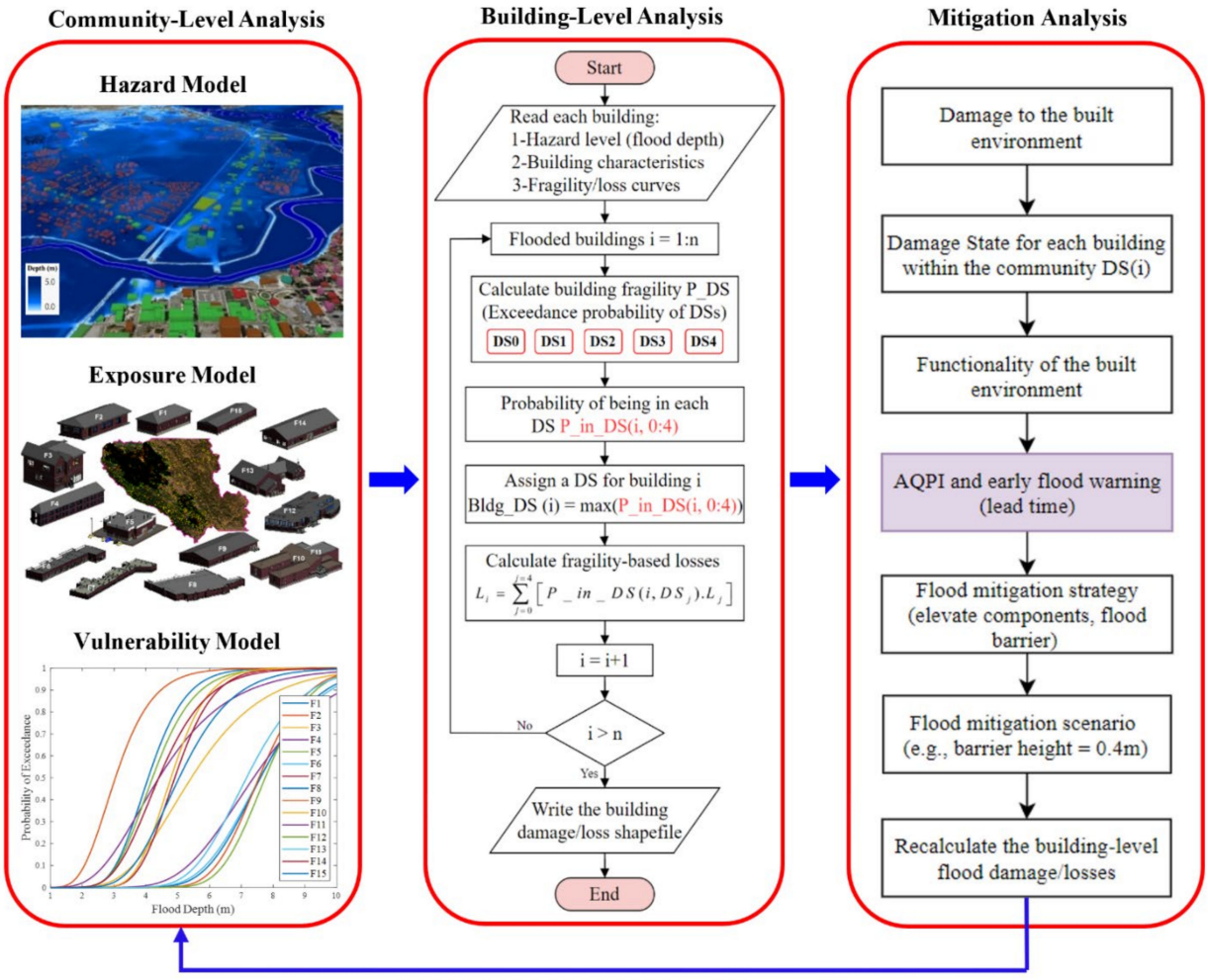

Figure 3. A schematic flow chart showing the main analysis steps for the flood risk and mitigation analysis.

Table 3 provides detailed information about the damage scale and the loss ratio along with the anticipated functionality level associated with each DS and more details about the description of each DS are provided in [43]. For post-hazard functionality assessment, buildings with more than 50% exceedance probability of DS2 are considered nonfunctional. Buildings with DS0 (insignificant damage) and DS1 (slight damage) can be easily returned to functionality in a few days after the flooding event but buildings with DS2 or higher would likely require a much longer time to return to normal functionality. This is because most of the appliances and the furniture will need to be replaced and drywall repair along with many other repairs to the electrical and mechanical systems which would require a lot of time and money.

Table 3. Anticipated functionality level associated with each damage state along with their damage scale and loss ratio [43].

DS Level	Functionality	Damage Scale	Loss Ratio
DS0	Operational	Insignificant	0.00–0.03
DS1	Limited Occupancy	Slight	0.03–0.15
DS2	Restricted Occupancy	Moderate	0.15–0.50
DS3	Restricted Use	Extensive	0.50–0.70
DS4	Restricted Entry	Complete	0.70–1.00

2.4. Building-Level Flood Mitigation Analysis

The early flood warnings provided by the AQPI system may enable more rapid mitigation actions at the household and stakeholder level. For households, there are a number of rapid mitigation actions such as elevating water-sensitive components (e.g., appliances, electronics, valuable items, and some furniture), moving vehicles to a higher elevation, and constructing a temporary barrier system around the property as shown schematically in Figure 4. Many of these mitigation measures can be performed in less than six hours which is within the range of the lead time provided by the AQPI system. For stakeholders, some other mitigation actions can be implemented to reduce the hazard severity and the exposure of community assets in the flood plain. These measures include early evacuation, improved reservoir management to release water, patching critical locations on creeks that can be a source of flooding and placement of pumps in locations that may flood (lower lands).

The impact of elevating some water-sensitive components was calculated by reconstructing the fragility and the loss functions using the new elevation of the components. This mitigation action was only investigated for residential buildings because it is not practical to apply it for commercial buildings. The damage analysis methodology that was used to reconstruct these fragility functions is fully described in these publications [44,47]. Table 4 provides detailed information of the select components including the old and new elevation and the replacement cost of these components for archetype F2 (a four-unit one-story multi-family residential building). Heavy appliances and furniture (e.g., washer, dryer, couches, etc.) are assumed to be elevated by 0.6 m (2 ft) from the ground and the lightweight valuable items (e.g., computers, electronics, counter items, etc.) are assumed to be elevated to the attic floor which is more than 3.0 m (9 ft) height from the first-floor elevation (FFE). Figure 5 shows the resulting flood fragility and loss functions for the residential building archetypes. For the one-story archetypes (F1 and F2), the resulting fragilities show that elevating the chosen components will slightly impact the calculated damage in terms of the exceedance probability of DS2 and DS3 and the loss curves as shown in Figure 5b,d with a flood loss reduction ranging from 3% to 10% depending on the flood depth. Although the amount of loss reduction looks insignificant and very little at the building level, it can be substantial at the community level.

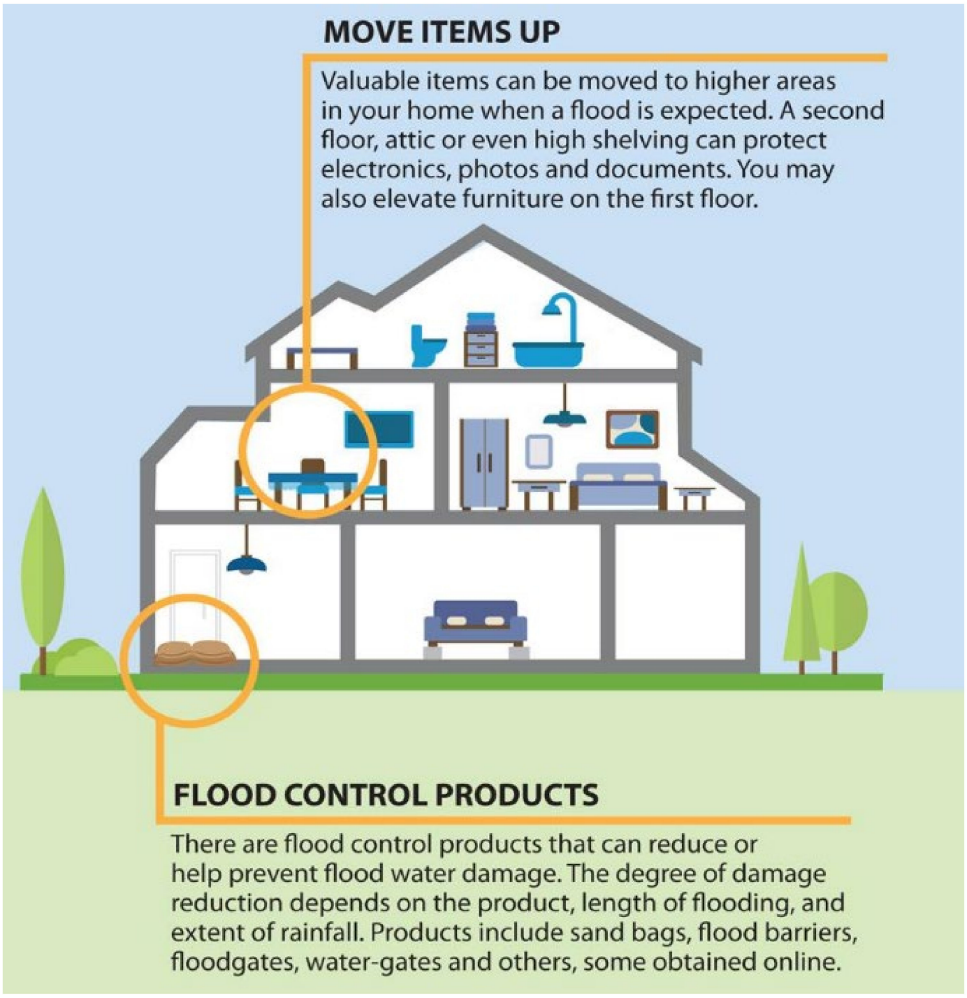

Figure 4. A schematic representation for a building with elevated content and front-door flood barrier.

Table 4. The mean and standard deviation of the old and new damaging elevation of the water-sensitive components along with their replacement cost.

Component	DS	Old-Elevation (m)		New-Elevation (m)		Component Cost (USD) *	
		μ	σ	μ	σ	μ	σ
Washer	DS2	0.15	0.05	0.75	0.05	3700	1150
Dryer		0.15	0.05	0.75	0.05	3700	1150
TV		1.05	0.23	3.4	0.2	2400	800
Speakers		0.05	0.65	3.4	0.2	2400	800
Bedroom		0.3	0.125	0.9	0.125	26,400	8400
Sofa and couches		0.3	0.125	0.9	0.125	24,800	7600
Chairs set		0.45	0.075	1.05	0.075	4600	1300
Desks		0.45	0.175	1.05	0.175	1400	300
TV mount/stand		0.35	0.15	0.95	0.15	4400	1800
Mixers	DS3	1.15	0.13	3.4	0.2	660	270
Microwave		1.15	0.13	3.4	0.2	1100	250
Computer		0.5	0.23	3.4	0.2	6600	2700
Laptop		0.5	0.23	3.4	0.2	6600	2700
Printer		0.5	0.2	3.4	0.2	500	150
Window AC Units		0.75	0.13	3.2	0.1	1100	250

* The replacement cost is in USD for archetype F2 which is a one-story multi-family building with four units. Therefore, the component cost is multiplied by four to include all the components.

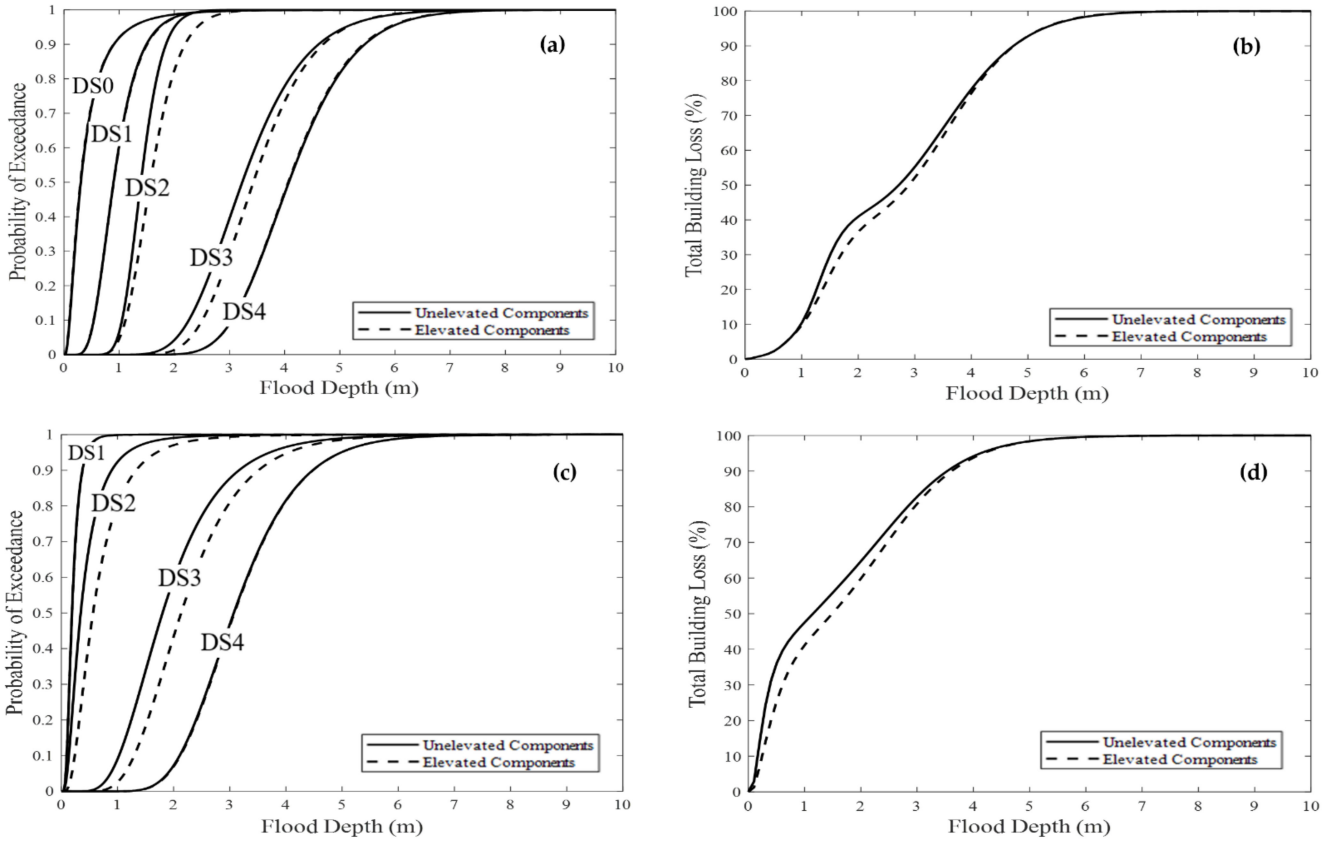

Figure 5. The fragility and loss functions based elevated and unelevated components for: (**a**,**b**) Archetype F1; (**c**,**d**) Archetype F2, respectively.

Temporary flood barriers are also considered a relatively rapid mitigation measure given the current advances in flood barrier systems including bladder dams, flood shields, box-walls, aquafences along with many other innovative flood barrier systems as illustrated in Figure 6. The sandbag system is considered one of the oldest flood barrier systems but it requires time, manpower, and sand in place for construction which would be unlikely to be able to be installed with only a few hours of lead time. On the other hand, other manufactured flood barriers require only a few hours depending on the barrier type and personnel resources to set it up. Figure 7 shows flood fragility functions for archetype F2 before and after using a flood barrier of 1.0 m height. More details about the impact of using a flood barrier on flood fragility and loss functions can be found in the literature [47]. The fragility function with a flood barrier simply accounts for zero flood damage if the flood depth is less than the barrier height assuming there is no leakage or returning flow from the sewers. If the flood depth exceeds the barrier height, the flood damage is calculated using the original fragility.

Figure 6. Different types of flood barrier systems.

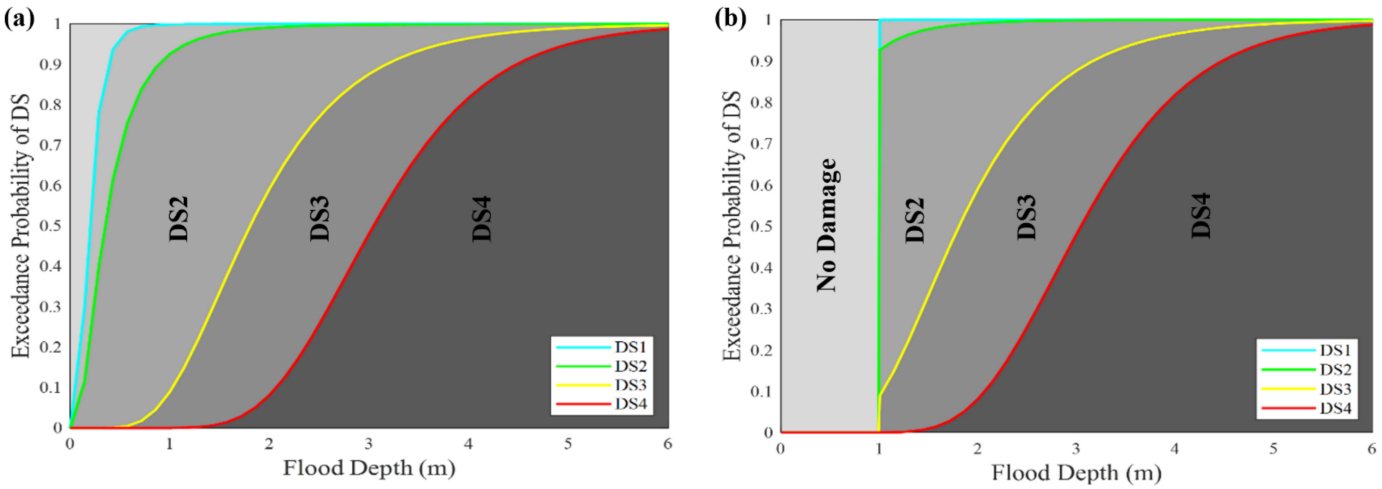

Figure 7. Fragility functions with and without flood barrier with a height of 1.0 m for a one-story multi-family residential building (F2): (**a**) Fragility curves without using a flood barrier; (**b**) fragility curves with the 1.0 m flood barrier.

3. Example Community: Santa Clara County, CA

3.1. Geographical Location and Demographics

Santa Clara County is one of the most populous counties in the U.S. (6th most populous) with almost two million people according to the 2010 census [53]. Santa Clara County is diverse with 37% of the population identifying as non-Hispanic Asian, 30.9% as non-Hispanic White, 23% as Hispanic, 2.8% as black or African American, while the other 6.3% are identified as multiracial groups [53]. Santa Clara County is an economic center for multiple industries and technology centers and has the third-highest GDP per capita in the world. The mean annual household income is USD 126,606 and the mean property value is USD 1.11M with more than a million employees. There are almost a half-million buildings within the County including housing units, commercial, industrial, and social institutions. Figure 8 shows the geographic location of Santa Clara County with respect to the State of California along with the spatial location of each building within the county. The tax assessor data for the whole county was used to identify building occupancy.

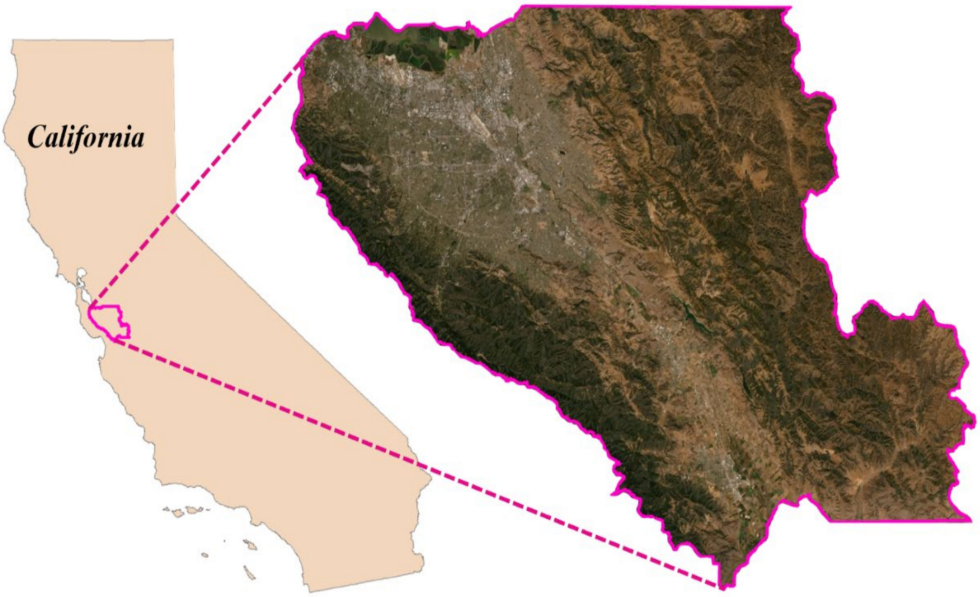

Figure 8. The geographic location of Santa Clara County with respect to the state of California.

3.2. Streams and Water Control Structures

Santa Clara County is surrounded by multiple bodies of water that feed the main streams within the floodplain. Figure 9 shows the main streams along with the location of eight main water control structures around Santa Clara County. In the northwest, Searsville Dam impounds Corte Madera Creek to form Searsville Lake and feeds San Francisquito Creek as shown in Figure 9a. In the west, Steven Creek Reservoir is formed by the Steven Creek Dam to feed two streams, Stevens Creek and Swiss Creek as shown in Figure 9b. Multiple lakes, retention ponds, and reservoirs are located on the Los Gatos Creek including Lexington Reservoir as shown in Figure 9c, Lake Elsman as shown in Figure 9d, Vasona Reservoir, and Camden Pond. In the south, Guadalupe Dam impounds multiple creaks (Rincon Creek, Guadalupe Creek, Los Capitancillos Creek) to form Guadalupe Reservoir to join them into one mainstream which is the Guadalupe Creek as shown in Figure 9e. Almaden Reservoir in the south was formed by the Almaden Dam after impounding Herbert Creek to feed Alamitos Creek as shown in Figure 9f. Calero Reservoir in the south was formed by the Calero Dam to feed Arroyo Calero Stream as shown in Figure 9g. In the southeast, Anderson Lake was formed by Anderson Dam to feed one of the largest streams in the area namely, Coyote Creek as shown in Figure 9h.

3.3. Flood Hazard Mapping

A scenario-based flood hazard map was developed using a 1.5 m high-resolution DEM. Most all of the streams have a controlled water flow by the upstream water control structures. Although a 100-year flood hazard map was developed using HAZUS-MH [50] as shown in Figure 10, the resulting hazard intensity with an average flood depth of 0.5 m was not high enough to reflect the significance of applying the proposed vulnerability mitigation methodology. Moreover, the resolution of the DEM (10 m) used to develop this hazard map was not high enough to capture enough details in the study area. On the other hand, a full hydrodynamic analysis using HEC-RAS would allow to include multiple hazard control measures. However, modeling a real flooding event for this area using HEC-RAS (e.g., the February 2017 flooding event) would require a detailed hydrologic analysis, which is doable, but it requires detailed information related to the reservoir management during the event in terms of the released discharges, which is not published. This is because all the upstream water flow is controlled by dams on these reservoirs and the reservoir data are confidential. Therefore, a hypothetical flood scenario using synthetic hydrographs upstream was developed to model a high-intensity flood hazard scenario that could be

used as an input for the proposed methodology. Figure 11 shows the simulated hazard map for the hypothetical flooding event along with close-up views on some locations within the study area.

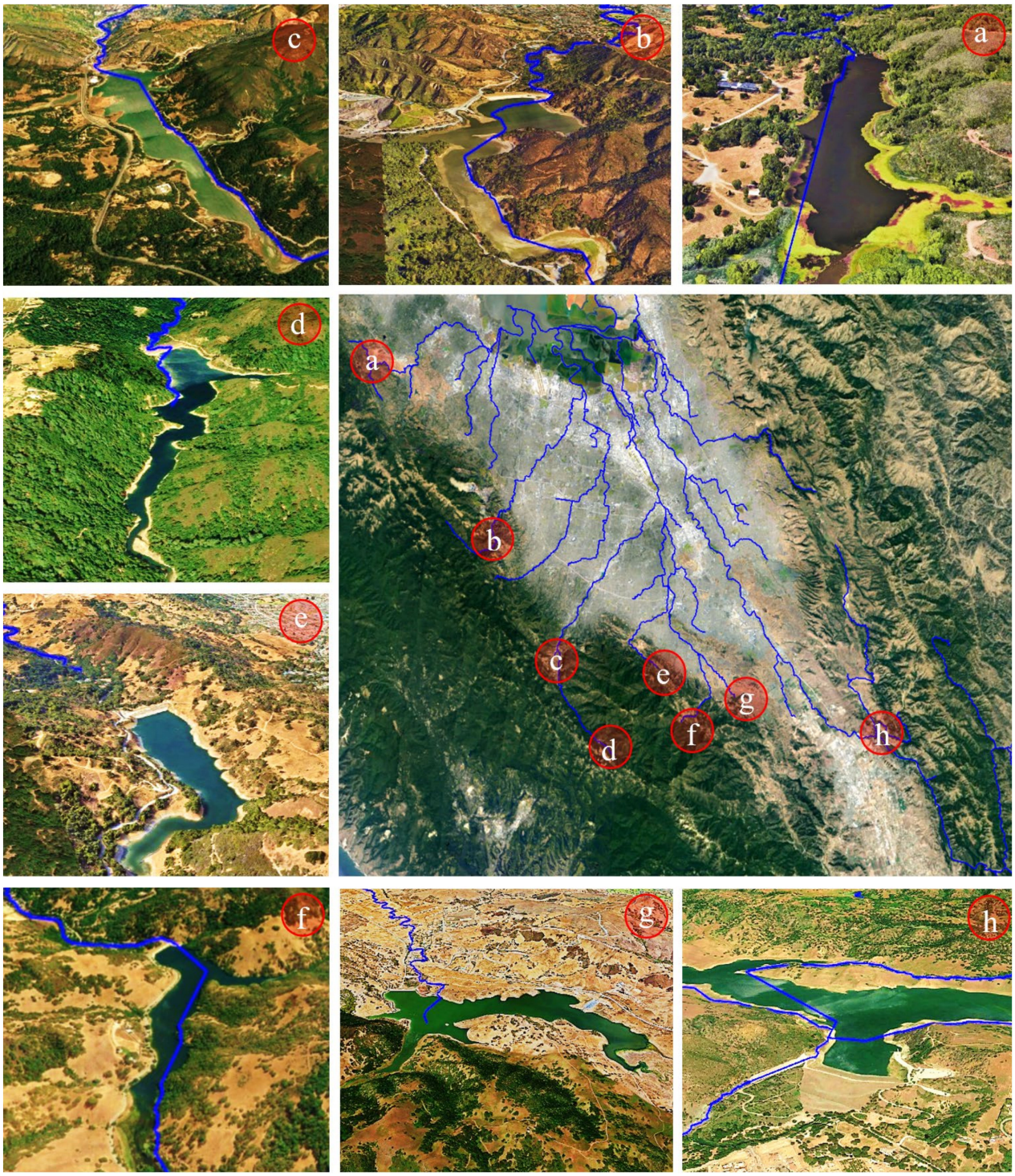

Figure 9. The main streams along with the location of the water control structures with respect to the Santa Clara County.

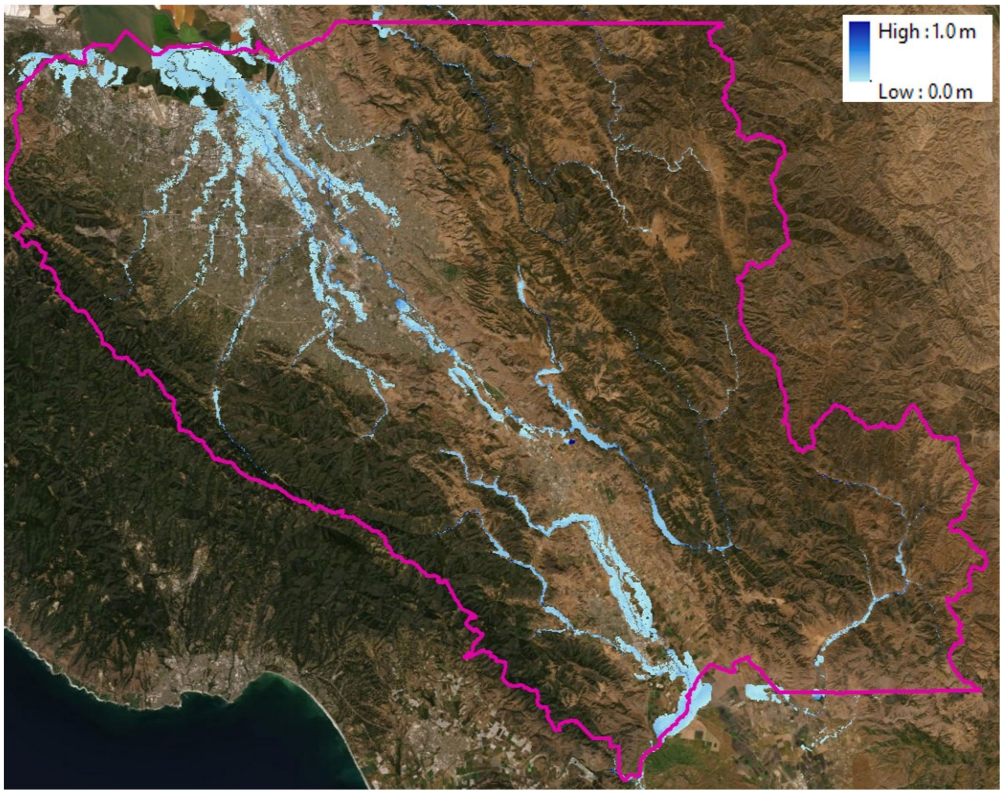

Figure 10. 100 yr flood hazard map for Santa Clara County based on HAZUS flood model.

For this simulation, synthetic hydrographs were used to model the output flow from the dams upstream. These synthetic hydrographs were developed by collecting data related to the discharge downstream from extreme flooding events and multiply it by a factor (1.3). This should not affect the integrity of this study as the main purpose is to investigate the mitigation of building vulnerability by elevating water-sensitive components or using flood barriers and not hazard mitigation. That is why using hypothetical hazard scenario was used as a baseline for damage analysis for buildings to be compared with the mitigation analysis results after using, e.g., flood barriers for the same hypothetical hazard intensity. These hydrographs are then used as boundary conditions in a hydrodynamic analysis to account for the flood hazard characteristics (e.g., flood depth, flood velocity, flood duration). HEC-RAS is a hydrodynamic computational environment developed by the U.S. Army Corps of Engineers [51] which was used to develop flood hazard maps. As a brief background, HEC-RAS is a computational environment that uses finite volume to solve the 2D Saint-Venant shallow water flow equations to calculate the flood hazard characteristics (e.g., depth, velocity, duration, etc.) for a predefined computational domain. A small mesh size of 20.0 m $\times$ 20.0 m was utilized to model the 2D computational domain. The level of detail used in the flood hazard mapping including the DEM resolution and the mesh size of the computation domain enabled the development of a detailed flood hazard map as shown in Figure 11. This includes small minor street flooding and floodwater movement from one street to another.

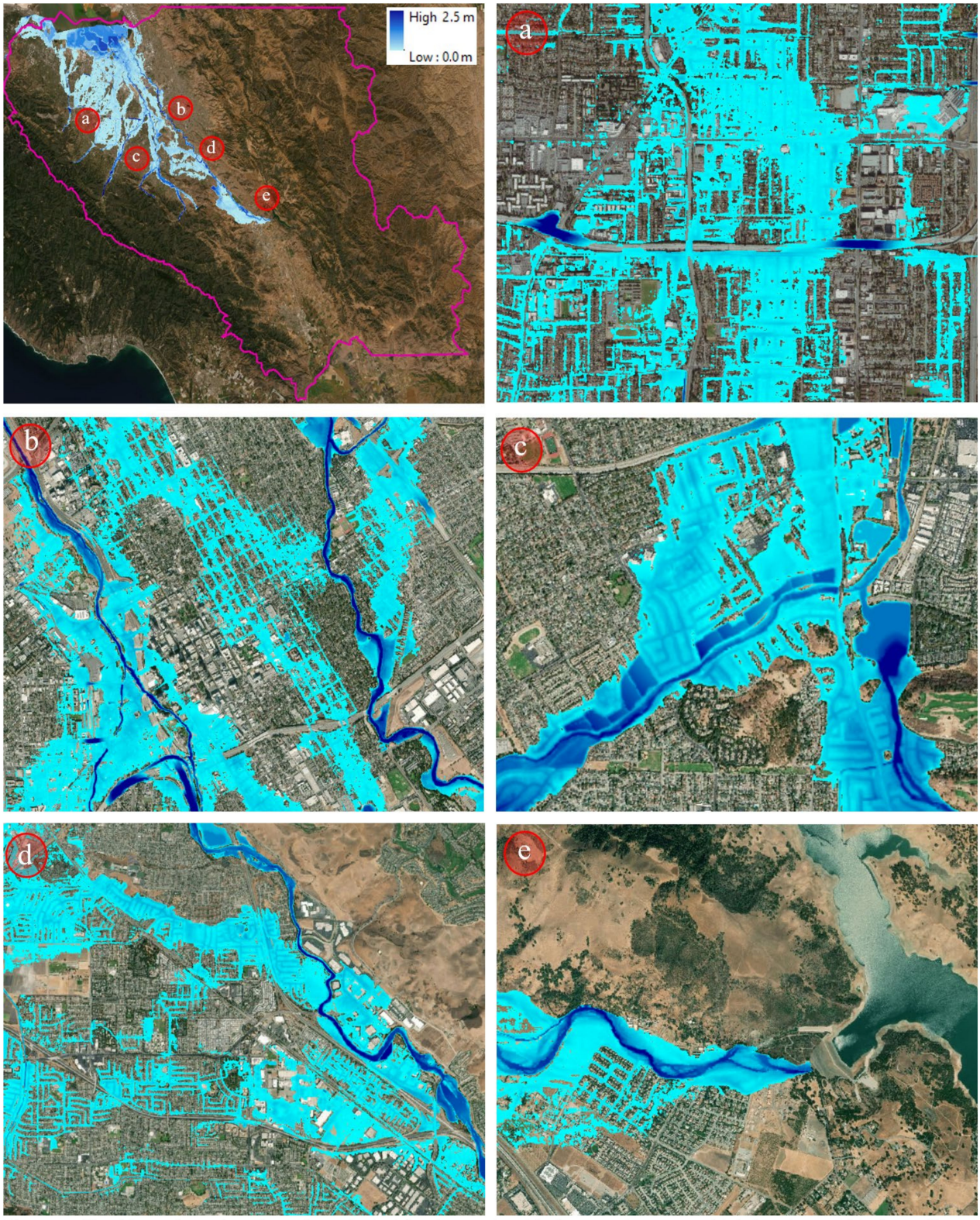

Figure 11. Flood hazard map based on a hypothetical flood scenario with close-up views on multiple locations within Santa Clara County as shown in (**a**–**e**).

3.4. Community Model

Although building data for Santa Clara County is not available online, third-party tax assessor data was purchased [48] which provided detailed building information about all parcels within the county. The parcel data was then assigned to the buildings using the mapping algorithm described earlier. This algorithm was applied to map the building archetypes to each of the 491,000 buildings within the community. Figure 12 shows a color-coded map based on the building archetypes for Santa Clara County with a schematic 3D view for each building archetype. The mapping algorithm showed high efficiency in terms of reducing the 400 building typologies provided by the tax assessor database to the 15 building archetypes from the portfolio as shown in the close-up views in Figure 12. The fragility functions associated with each building archetype were then assigned to each building within the community to initiate the flood vulnerability analysis.

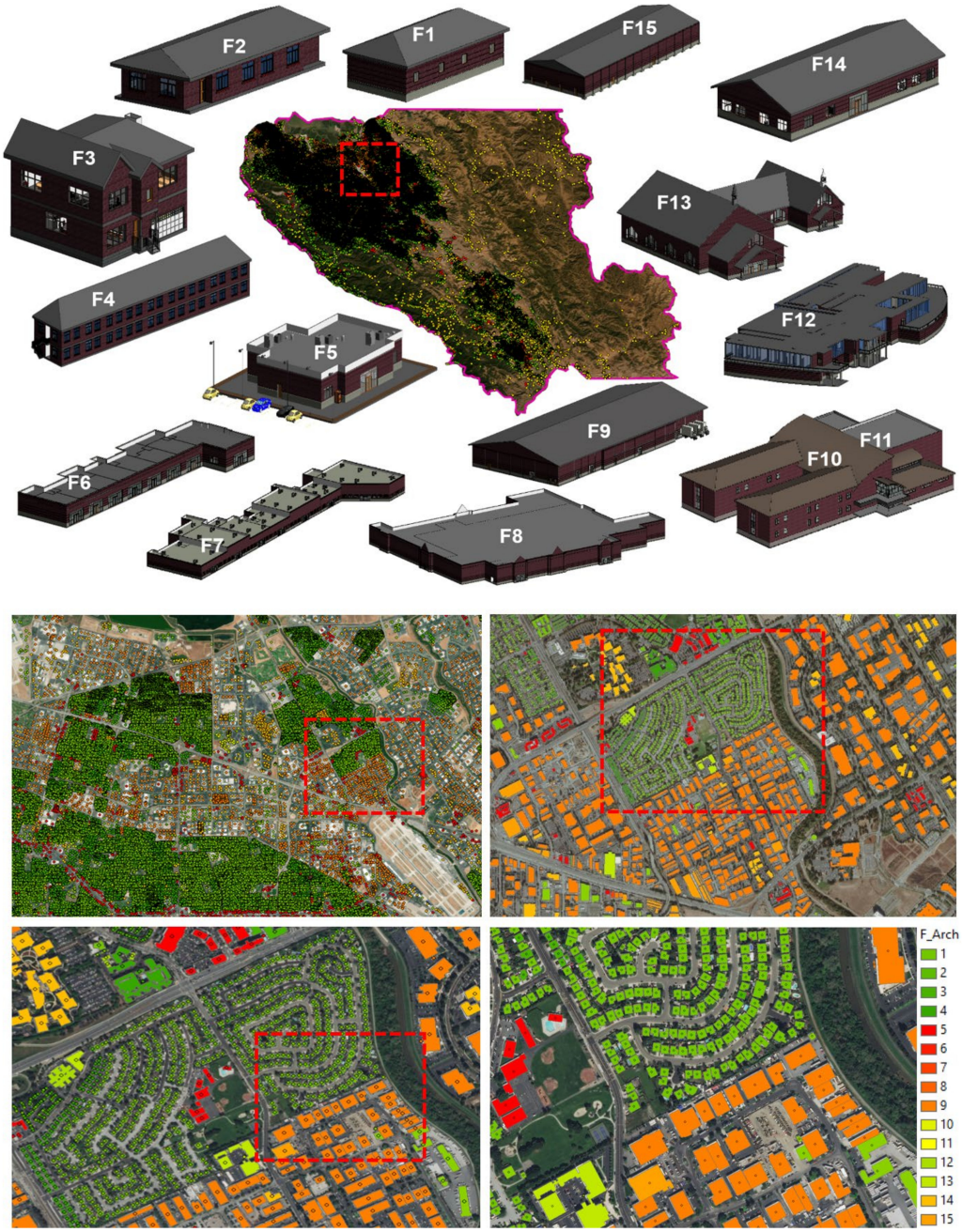

Figure 12. Schematic representation of the Santa Clara County color-coded based on the 15 building archetypes portfolio with close-up views on select locations.

4. Results

The hazard map was overlaid with the community model in a GIS environment to identify all the exposed buildings as shown in Figure 13. The number of buildings within the floodplain associated with the hypothetical scenario was 43,832 buildings out of the total 491,000 buildings within the County. The analysis was only conducted on the buildings in the floodplain which received flood depth above the ground elevation (GE). However, many of the exposed buildings in the floodplain were not damaged because the FFE was more than GE and the water surface elevation (WSE). As discussed earlier, the direct flood losses were calculated to identify the impact of the building-level flood mitigation measures using the early flood warning provided by the AQPI system. Therefore, the original flood fragility functions were used first to account for the flood losses without early flood warnings, i.e., the benchmark analysis. Then, another set of flood loss analyses was conducted using the reduced fragility functions corresponding to each mitigation measure (elevate water-sensitive components, flood barriers). Afterwards, the calculated flood damage was used to account for the functionality of each building in the flood plain.

Figure 13. A 3D view for the Santa Clara County with buildings color-coded based on their archetypes and overlaid with the flooding (hazard) layer to identify the exposed buildings with close-up views on one of the flooded locations.

4.1. Flood Losses without Early Flood Warnings (without AQPI)

The physical damage for each impacted building was calculated in terms of the exceedance probability of each DS. Table 5 provides the exceedance probability of each DS for all the 43,832 buildings in the floodplain in terms of six ranges from 0% to 100% exceedance probability. For example, there are 1451 buildings with more than a 40% exceedance probability of DS2. For loss analysis, a DS was assigned for each building based on the maximum probability of being in each DS using Equation (1). Figure 14 shows a color-coded map based on buildings assigned DS for the buildings in the floodplain only along with close-up views on multiple locations within the flooded areas and the number of total buildings within each DS is in the legend of Figure 14. Then, the total fragility-based flood loss for each building was calculated by multiplying the probability of being in each DS by the replacement/repair cost associated with each DS using Equation (2). Figure 15a shows a color-coded map based on the fragility-based losses for one of the flooded locations. Although more than 43,000 buildings are identified as being in the floodplain for Santa Clara County, the flood depth for the majority of these buildings is less than the FFE. This means that streets were flooded as shown in Figure 14, but the water was not able to breach inside the buildings, or only the crawlspace was flooded if the building had a crawlspace foundation. Recall buildings are assumed nonfunctional if they have more than a 50% exceedance probability of DS2. The analysis results showed that there are more than 37,000 buildings in the floodplain are identified as DS0 (34,396 buildings) and DS1 (2726 buildings). These buildings are considered functional because it takes only a few days after the flooding event to repair the damage, or at least be/remain inhabitable. On the other hand, the analysis results showed that there are more than 6000 buildings that were identified as nonfunctional as shown in Figure 15b.

Table 5. Damage states exceedance probability corresponding to each flood-induced hazard for the exposed buildings within the County of Santa Clara.

Exceedance Probability of Each DS (Fragility)	Number of Buildings (Total = 43,832)				
	DS0	DS1	DS2	DS3	DS4
P_DS = 0%	17,262	25,035	31,419	39,387	42,851
0% < P_DS < 20%	8662	6335	3751	3097	724
20% < P_DS < 40%	4930	1852	1735	604	116
40% < P_DS < 60%	3967	1450	1451	332	33
60% < P_DS < 80%	3533	1661	1510	269	34
80% < P_DS < 100%	5478	7499	3966	143	74

4.2. Flood Losses with Early Flood Warnings (with AQPI)

Another set of analyses was conducted after using the modified fragility functions that account for the increased elevation of water-sensitive made possible by early flood warnings provided by the AQPI system. However, to be realistic, not all households will be able to either elevate their water-sensitive components or set up a flood barrier system. Therefore, the analysis was conducted based on a percentage of households complying and reacting to the warning based on the total number of buildings (e.g., 10%, 20%, . . . , 100%). The actual buildings corresponding to each ratio were selected randomly from all the buildings in the floodplain. Some of these ratios are likely closer to reality with good public messaging (e.g., 20%, 30%) and other ratios are hypothetical for comparisons only (e.g., 90%, 100%). The amount of community-level flood loss reduction and the number of nonfunctional buildings corresponding to each response ratio was calculated. The analysis results showed that if 50% of the households in the floodplain were able to elevate their water-sensitive components, a food loss reduction of 6% could be achieved with a decrease of 400 for a number of nonfunctional buildings. Figure 16 shows the impact of elevating water-sensitive components on the amount of flood loss reduction and the decrease in the number of nonfunctional buildings corresponding to each response ratio.

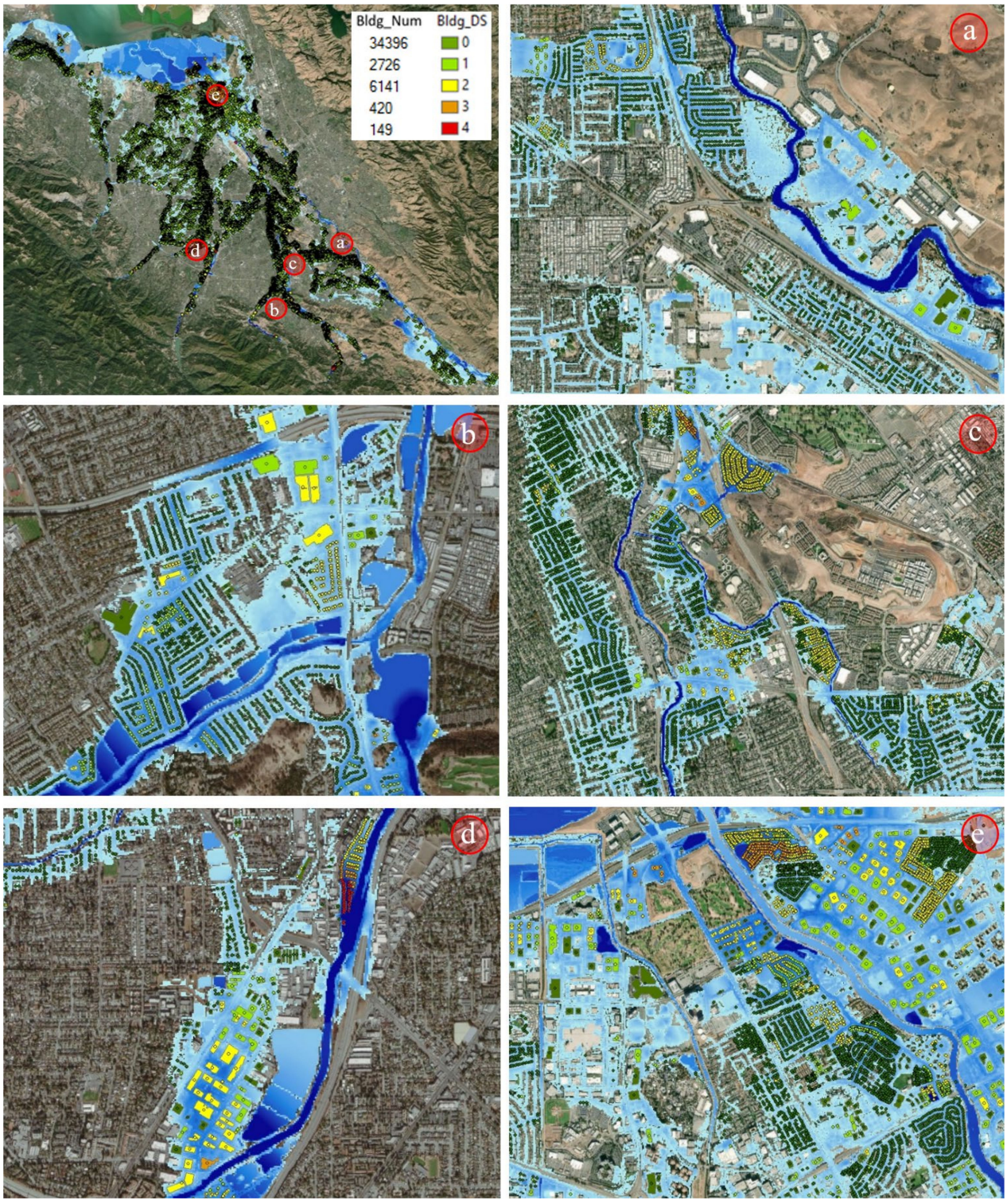

Figure 14. A color-coded map for Santa Clara County based on buildings damage states with close-up views on multiple locations as shown in (**a**–**e**).

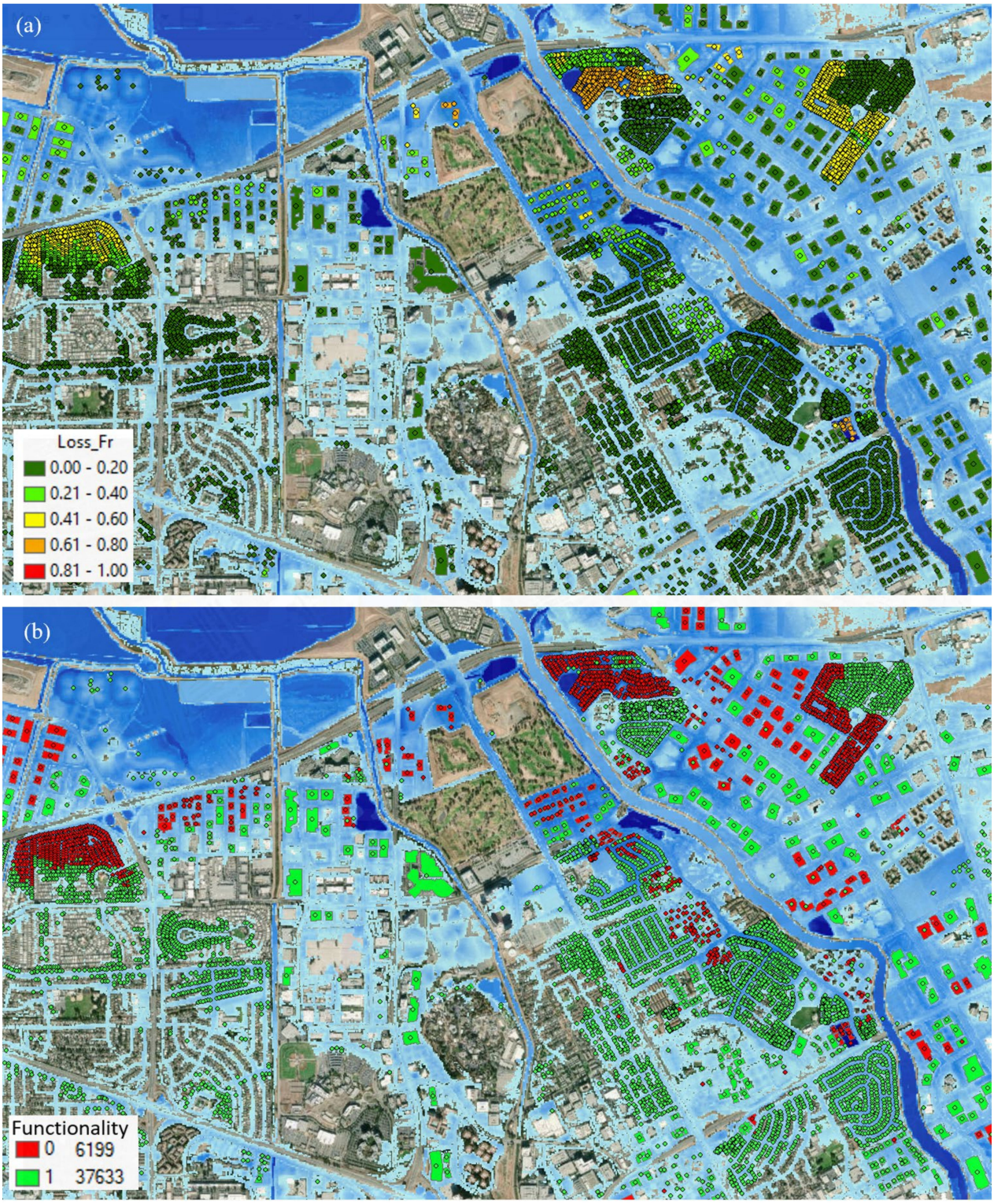

Figure 15. Color-coded maps for one of the flooded locations: (**a**) Color-coded buildings based on the buildings' functionality after the flooding event (red: unfunctional, green: functional); (**b**) color-coded buildings based on the amount calculated flood losses.

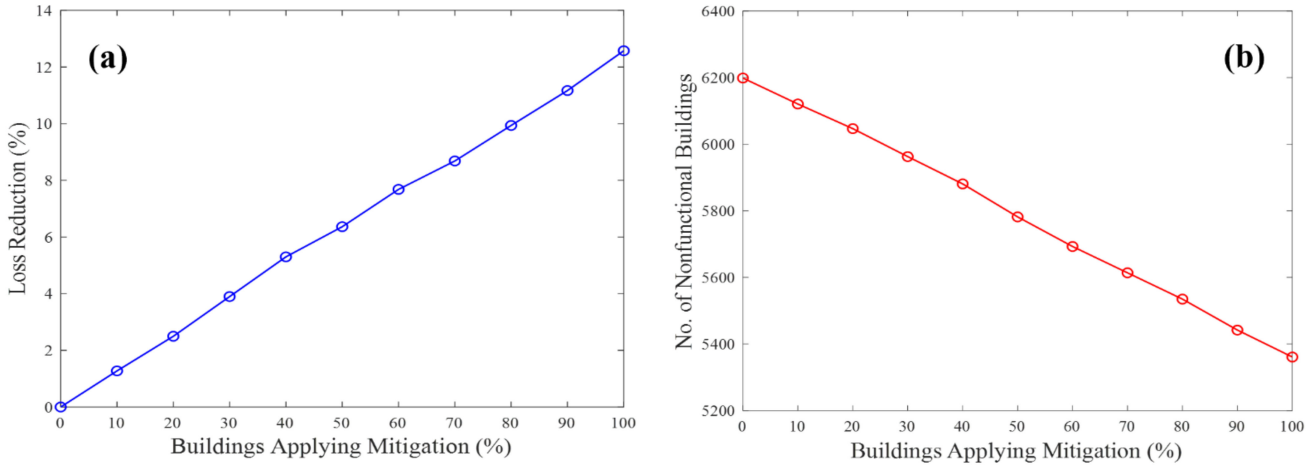

Figure 16. The impact of elevating water-sensitive components corresponding to each response ratio on: (**a**) The amount of flood loss reduction; (**b**) the number of nonfunctional buildings. corresponding to each response ratio.

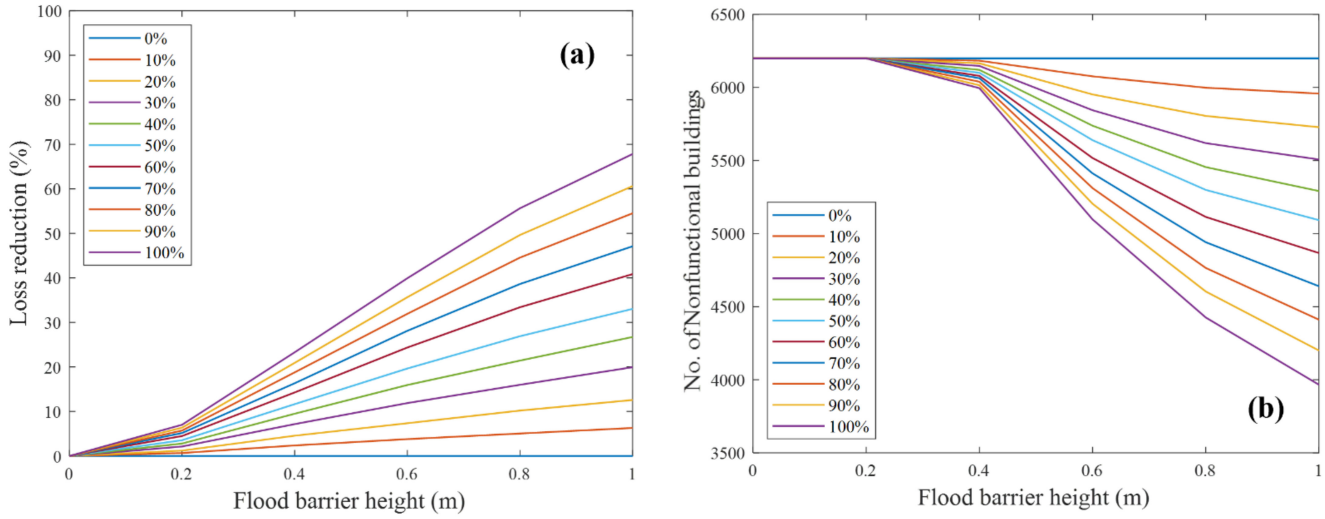

Figure 17. The impact of using flood barriers for all building occupancies using different barrier height corresponding to each response ratio on: (**a**) The percentage of flood loss reduction; (**b**) The number of nonfunctional buildings.

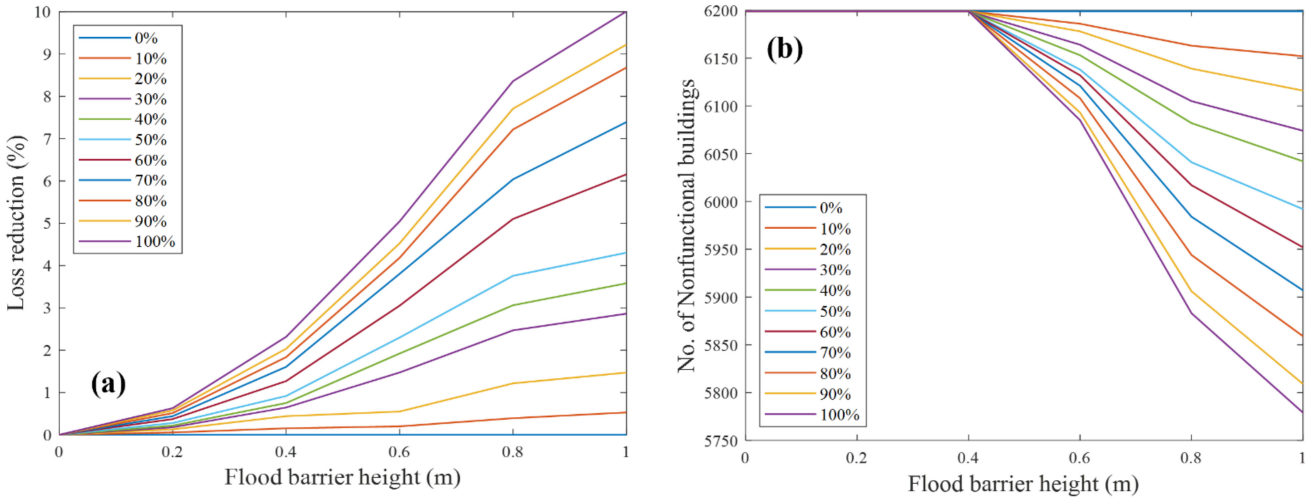

Figure 18. The impact of using flood barriers for commercial buildings only using different barrier height corresponding to each response ratio on: (**a**) The percentage of flood loss reduction; (**b**) The number of nonfunctional buildings.

Although the percentage of the flood loss reduction corresponding to increasing the elevation of the water-sensitive components is very low, it is still a considerable amount of savings for the households' assets within the floodplain. Additionally, the decrease in the number of nonfunctional buildings will decrease the amount of indirect economic losses, i.e., dislocation, loss of work, etc. It should be noted that elevating water-sensitive components was only applied to residential buildings within each of the scenarios, i.e., the ratio of those complying. Recall the flood barriers discussed earlier. A similar approach was used for this community-level analysis by assuming some percentages of buildings would/could comply. The analysis results showed that if 20% of all the buildings (including residential and commercial buildings) in the floodplain were able to construct a flood barrier of 1.0 m height, the flood losses will be reduced by almost 13% and the number of nonfunctional buildings would be reduced by 430 buildings. Although this may not be realistic, it provides some insight into mitigation strategy. Figure 17 shows the impact of using a number of barrier heights corresponding to different building response ratios on the amount of flood loss reduction and the decrease in the number of nonfunctional buildings. Setting up a barrier system would likely be a burden for a residential building, but it could be financially possible for many commercial buildings. Therefore, separate mitigation simulations were conducted using flood barriers for commercial buildings only. The analysis results showed that if 50% of the commercial buildings in the flood plain were able to construct a flood barrier of a 1.0 m height, the flood losses will be reduced by 4.3% and the number of nonfunctional buildings could be reduced by 220 buildings as shown in Figure 18.

5. Discussion

The analysis results from more than 100 mitigation simulations at the component and building level revealed that soft mitigation interventions such as elevating water-sensitive components and using flood barriers can result in a significant savings of thousands of dollars at the building level and millions of dollars at the community level. This means that some mitigation interventions beyond large-scale hazard mitigation measures can provide a significant amount of flood loss reduction if a proper early flood warning system is implemented. This emphasizes the novelty of this approach in that it can provide a quantitative assessment of such mitigation intervention at the component and building level to inform the amount of flood loss reduction at the community level using a high-resolution flood risk model. For example, the level of detail is such that the method can quantify the effect of raising an electronic device one meter off the ground in 20% of the buildings within a community. However, it is important to address the inherent limitations within each part of the methodology which includes:

- The study area would need to implement the AQPI system to have a lead time before severe rainfall events such that it allows implementing rapid mitigation interventions.
- Detailed information about the buildings within the community is needed to develop the high-resolution community model and the vulnerability analysis accuracy depends on how the buildings within the community match the 15 building archetypes. For example, high-rise buildings are not included in the suite of archetypes since the authors did not develop vulnerability functions for them.
- Synthetic hydrographs were used to develop the flood hazard maps due to the confidentiality of the ground truth hydrographs. This study would be more realistic if the exact upstream hydrographs were used to model the realistic flood hazard event.
- Since the investigated mitigation interventions depend on the physical and financial ability of household or business owners to implement these specific mitigation measures, the applied updated fragility functions used in this paper are conditioned on the implementation of these measures. That is why the authors investigated different percentages of the households that could apply these mitigation measures.

6. Summary and Conclusions

A high-resolution flood risk analysis approach was developed to account for the direct flood losses at the community level and used to identify the impact of early flood warnings using the AQPI system on the amount of flood loss reduction for buildings across a large example community. Two mitigation measures were investigated which focused on household actions that could be done within a few hours of lead time before a flooding event. The model was applied to the example community of Santa Clara County, California. A hypothetical flood hazard scenario was developed for Santa Clara County. Detailed building information was then used to model the community based on a new mapping algorithm to map 15 building archetypes to the real community. Then, a fragility-based flood damage analysis was conducted using a flood damage analysis algorithm that overlays the hazard data with the building data in a GIS environment to identify the exposed buildings and the hazard intensity at each building. Finally, the amount of damage was quantified by calculating the exceedance probability of each DS using the fragility function associated with each building archetype. The high-resolution model enabled a quantitative analysis of the direct flood losses to the buildings in the floodplain. The resolution of the model, namely at the component level, allowed investigation of mitigation strategies at the individual building level to be propagated to the community level. Such an approach can provide reliable risk-informed decision support to identify the feasibility of mitigation strategies and enhance community resilience. The mitigation strategies made possible by the AQPI technology marginally reduce losses from flooding at the individual building level, but when aggregated to a community level for a large community can be financially sizable.

Author Contributions: Conceptualization, O.M.N. and J.W.v.d.L.; data curation: K.C.; methodology, O.M.N. and J.W.v.d.L.; software, O.M.N.; formal analysis, O.M.N.; writing—original draft preparation, O.M.N.; writing—review and editing, O.M.N. and J.W.v.d.L., H.C. and M.S.; supervision, J.W.v.d.L.; project administration, J.W.v.d.L.; funding acquisition, H.C. All authors have read and agreed to the published version of the manuscript.

Funding: This work was supported by the National Oceanic and Atmospheric (NOAA) Office of Oceanic and Atmospheric Research (OAR), and the NOAA Earth System Research Laboratory (ESLR) Physical Science Division under grant No. NA19OAR4320073. The findings and conclusions of this research are those of the authors and do not necessarily represent the views of NOAA.

Institutional Review Board Statement: Not applicable.

Informed Consent Statement: Not applicable.

Data Availability Statement: The data presented in this study are available on request from the corresponding author.

Conflicts of Interest: The authors declare no conflict of interest.

References

1. Mallakpour, I.; Villarini, G. Investigating the Relationship between the Frequency of Flooding over the Central United States and Large-Scale Climate. *Adv. Water Resour.* **2016**, *92*, 159–171. [CrossRef]
2. Dottori, F.; Szewczyk, W.; Ciscar, J.-C.; Zhao, F.; Alfieri, L.; Hirabayashi, Y.; Bianchi, A.; Mongelli, I.; Frieler, K.; Betts, R.A. Increased Human and Economic Losses from River Flooding with Anthropogenic Warming. *Nat. Clim. Chang.* **2018**, *8*, 781–786. [CrossRef]
3. Chou, J.; Xian, T.; Dong, W.; Xu, Y. Regional Temporal and Spatial Trends in Drought and Flood Disasters in China and Assessment of Economic Losses in Recent Years. *Sustainability* **2019**, *11*, 55. [CrossRef]
4. Barredo, J.I. Normalised Flood Losses in Europe 1970–2006. *Nat. Hazards Earth Syst. Sci.* **2009**, *9*, 97–104. [CrossRef]
5. Tezuka, S.; Takiguchi, H.; Kazama, S.; Sato, A.; Kawagoe, S.; Sarukkalige, R. Estimation of the Effects of Climate Change on Flood-Triggered Economic Losses in Japan. *Int. J. Disaster Risk Reduct.* **2014**, *9*, 58–67. [CrossRef]
6. Dottori, F.; Figueiredo, R.; Martina, M.L.; Molinari, D.; Scorzini, A. INSYDE: A Synthetic, Probabilistic Flood Damage Model Based on Explicit Cost Analysis. *Nat. Hazards Earth Syst. Sci* **2016**, *16*, 2577–2591. [CrossRef]
7. Thieken, A.H.; Ackermann, V.; Elmer, F.; Kreibich, H.; Kuhlmann, B.; Kunert, U.; Maiwald, H.; Merz, B.; Müller, M.; Piroth, K.; et al. Methods for the Evaluation of Direct and Indirect Flood Losses. In Proceedings of the 4th International Symposium on Flood Defence: Managing Flood Risk, Reliability and Vulnerability, Toronto, ON, Canada, 6–8 May 2008; pp. 6–8.

8. De Moel, H.; Aerts, J.C.J.H. Integrated Direct and Indirect Flood Risk Modeling: Development and Sensitivity Analysis. *Risk Anal.* **2015**, *35*, 882–900.
9. Carrera, L.; Standardi, G.; Bosello, F.; Mysiak, J. Assessing Direct and Indirect Economic Impacts of a Flood Event through the Integration of Spatial and Computable General Equilibrium Modelling. *Environ. Model. Softw.* **2015**, *63*, 109–122. [CrossRef]
10. Kuriqi, A.; Hysa, A. Multidimensional Aspects of Floods: Nature-Based Mitigation Measures from Basin to River Reach Scale. In *The Handbook of Environmental Chemistry*; Springer: Berlin/Heidelberg, Germany, 2021.
11. Apel, H.; Aronica, G.T.; Kreibich, H.; Thieken, A.H. Flood Risk Analyses—How Detailed Do We Need to Be? *Nat. Hazards* **2009**, *49*, 79–98. [CrossRef]
12. McGrath, H.; Stefanakis, E.; Nastev, M. Sensitivity Analysis of Flood Damage Estimates: A Case Study in Fredericton, New Brunswick. *Int. J. Disaster Risk Reduct.* **2015**, *14*, 379–387. [CrossRef]
13. Thieken, A.; Merz, B.; Kreibich, H.; Apel, H. Methods for Flood Risk Assessment: Concepts and Challenges. In Proceedings of the International Workshop on Flash Floods in Urban Areas, Muscat, Oman, 4–6 September 2006; pp. 1–12.
14. Merz, B.; Kreibich, H.; Schwarze, R.; Thieken, A. Review Article "Assessment of Economic Flood Damage". *Nat. Hazards Earth Syst. Sci.* **2010**, *10*, 1697–1724. [CrossRef]
15. Salman, A.M.; Asce, A.M.; Li, Y.; Asce, M. Flood Risk Assessment, Future Trend Modeling and Risk Communication: A Review of Ongoing Research. *Nat. Hazards Rev.* **2018**, *19*, 04018011. [CrossRef]
16. Nofal, O.M.; van de Lindt, J.W. Understanding Flood Risk in the Context of Community Resilience Modeling for the Built Environment: Research Needs and Trends. *Sustain. Resil. Infrastruct.* **2020**, *5*, 1–17. [CrossRef]
17. Díez-Herrero, A.; Garrote, J. Flood Risk Analysis and Assessment, Applications and Uncertainties: A Bibliometric Review. *Water* **2020**, *12*, 2050. [CrossRef]
18. Marvi, M.T. A Review of Flood Damage Analysis for a Building Structure and Contents. *Nat. Hazards* **2020**, *3*, 967–995. [CrossRef]
19. Seleem, O.; Heistermann, M.; Bronstert, A. Efficient Hazard Assessment for Pluvial Floods in Urban Environments: A Benchmarking Case Study for the City of Berlin, Germany. *Water* **2021**, *13*, 2476. [CrossRef]
20. Tariq, A.; Shu, H.; Kuriqi, A.; Siddiqui, S.; Gagnon, A.S.; Lu, L.; Linh, N.T.T.; Pham, Q.B. Characterization of the 2014 Indus River Flood Using Hydraulic Simulations and Satellite Images. *Remote Sens.* **2021**, *13*, 2053. [CrossRef]
21. Antony, R.; Rahiman, K.U.A.; Vishnudas, S. Flood Hazard Assessment and Flood Inundation Mapping—A Review. In *Current Trends in Civil Engineering*; Thomas, J., Jayalekshmi, B.R., Nagarajan, P., Eds.; Springer: Berlin/Heidelberg, Germany, 2021; pp. 209–218.
22. Teng, J.; Jakeman, A.J.; Vaze, J.; Croke, B.F.W.; Dutta, D.; Kim, S. Flood Inundation Modelling: A Review of Methods, Recent Advances and Uncertainty Analysis. *Environ. Model. Softw.* **2017**, *90*, 201–216. [CrossRef]
23. Nkwunonwo, U.C.; Whitworth, M.; Baily, B. A Review of the Current Status of Flood Modelling for Urban Flood Risk Management in the Developing Countries. *Sci. Afr.* **2020**, *7*, e00269. [CrossRef]
24. Néelz, S.; Pender, G. *Benchmarking the Latest Generation of 2D Hydraulic Modelling Packages*; Environment Agency: Bristol, UK, 2013.
25. De Moel, H.; Aerts, J.C.J.H.; Koomen, E. Development of Flood Exposure in the Netherlands during the 20th and 21st Century. *Glob. Environ. Chang.* **2011**, *21*, 620–627. [CrossRef]
26. Röthlisberger, V.; Zischg, A.P.; Keiler, M. Identifying Spatial Clusters of Flood Exposure to Support Decision Making in Risk Management. *Sci. Total Environ.* **2017**, *598*, 593–603. [CrossRef] [PubMed]
27. Budiyono, Y.; Aerts, J.; Brinkman, J.; Marfai, M.A.; Ward, P. Flood Risk Assessment for Delta Mega-Cities: A Case Study of Jakarta. *Nat. Hazards* **2015**, *75*, 389–413. [CrossRef]
28. Scawthorn, C.; Asce, F.; Flores, P.; Blais, N.; Seligson, H.; Tate, E.; Chang, S.; Mifflin, E.; Thomas, W.; Murphy, J.; et al. HAZUS-MH flood loss estimation methodology. II. Damage and loss assessment. *Nat. Hazards Rev.* **2006**, *7*, 72–81. [CrossRef]
29. Amirebrahimi, S.; Rajabifard, A.; Mendis, P.; Ngo, T. A BIM-GIS Integration Method in Support of the Assessment and 3D Visualisation of Flood Damage to a Building. *J. Spat. Sci.* **2016**, *61*, 317–350. [CrossRef]
30. Ferguson, A.P.; Ashley, W.S. Spatiotemporal Analysis of Residential Flood Exposure in the Atlanta, Georgia Metropolitan Area. *Nat. Hazards* **2017**, *87*, 989–1016. [CrossRef]
31. Nofal, O.M.; van de Lindt, J.W. Probabilistic Flood Loss Assessment at the Community Scale: Case Study of 2016 Flooding in Lumberton, North Carolina. *ASCE-ASME J. Risk Uncertain. Eng. Syst. Part A Civ. Eng.* **2020**, *6*, 5020001. [CrossRef]
32. De Risi, R.; Jalayer, F.; De Paola, F.; Iervolino, I.; Giugni, M.; Topa, M.E.; Mbuya, E.; Kyessi, A.; Manfredi, G.; Gasparini, P. Flood Risk Assessment for Informal Settlements. *Nat. Hazards* **2013**, *69*, 1003–1032. [CrossRef]
33. Nadal, N.C.; Zapata, R.E.; Pagán, I.; López, R.; Agudelo, J. Building Damage Due to Riverine and Coastal Floods. *J. Water Resour. Plan. Manag.* **2009**, *136*, 327–336. [CrossRef]
34. Nofal, O.M.; van de Lindt, J.W.; Do, T.Q. Multi-Variate and Single-Variable Flood Fragility and Loss Approaches for Buildings. *Reliab. Eng. Syst. Saf.* **2020**, *202*, 106971. [CrossRef]
35. Figueiredo, R.; Romão, X.; Paupério, E. Component-Based Flood Vulnerability Modelling for Cultural Heritage Buildings. *Int. J. Disaster Risk Reduct.* **2021**, *61*, 102323. [CrossRef]
36. Van de Lindt, J.W.; Taggart, M. Fragility Analysis Methodology for Performance-Based Analysis of Wood-Frame Buildings for Flood. *Nat. Hazards Rev.* **2009**, *10*, 113–123. [CrossRef]
37. Afifi, Z.; Chu, H.-J.; Kuo, Y.-L.; Hsu, Y.-C.; Wong, H.-K.; Zeeshan Ali, M. Residential Flood Loss Assessment and Risk Mapping from High-Resolution Simulation. *Water* **2019**, *11*, 751. [CrossRef]

38. Armal, S.; Porter, J.R.; Lingle, B.; Chu, Z.; Marston, M.L.; Wing, O.E.J. Assessing Property Level Economic Impacts of Climate in the US, New Insights and Evidence from a Comprehensive Flood Risk Assessment Tool. *Climate* **2020**, *8*, 116. [CrossRef]
39. FEMA. Multi-Hazard Loss Estimation Methodology: Flood Model. In *HAZUS-MH MR4 Technical Manual*; Federal Emergency Management Agency: Washington, DC, USA, 2009.
40. De Moel, H.; Aerts, J.C.J.H. Effect of Uncertainty in Land Use, Damage Models and Inundation Depth on Flood Damage Estimates. *Nat. Hazards* **2011**, *58*, 407–425. [CrossRef]
41. Winter, B.; Schneeberger, K.; Huttenlau, M.; Stötter, J. Sources of Uncertainty in a Probabilistic Flood Risk Model. *Nat. Hazards* **2018**, *91*, 431–446. [CrossRef]
42. Van de Lindt, J.W.; Peacock, W.G.; Mitrani-Reiser, J.; Rosenheim, N.; Deniz, D.; Dillard, M.; Tomiczek, T.; Koliou, M.; Graettinger, A.; Crawford, P.S. Community Resilience-Focused Technical Investigation of the 2016 Lumberton, North Carolina, Flood: An Interdisciplinary Approach. *Nat. Hazards Rev.* **2020**, *21*, 4020029. [CrossRef]
43. Nofal, O.M.; Van de Lindt, J.W. Minimal Building Flood Fragility and Loss Function Portfolio for Resilience Analysis at the Community-Level. *Water* **2020**, *12*, 2277. [CrossRef]
44. Nofal, O.M.; Van de Lindt, J.W. High-Resolution Flood Risk Approach to Quantify the Impact of Policy Change on Flood Losses at Community-Level. *Int. J. Disaster Risk Reduct.* **2021**, *62*, 102429. [CrossRef]
45. Nofal, O.M.; van de Lindt, J.W. Fragility-Based Flood Risk Modeling to Quantify the Effect of Policy Change on Losses at the Community Level. *Civ. Eng. Res. J.* **2021**, *11*. [CrossRef]
46. Nofal, O.M. *High-Resolution Multi-Hazard Approach to Quantify Hurricane-Induced Risk for Coastal and Inland Communities*; Colorado State University: Boulder, CO, USA, 2021.
47. Nofal, O.M.; van de Lindt, J.W. High-Resolution Approach to Quantify the Impact of Building-Level Flood Mitigation and Adaptation Measures on Flood Losses at the Community-Level. *Int. J. Disaster Risk Reduct.* **2020**, *51*, 101903. [CrossRef]
48. Turner, G.; Said, F.; Afzal, U.; Campbell, K. The effect of early flood warnings on mitigation and recovery during the 2010 Pakistan floods. In *Reducing Disaster: Early Warning Systems for Climate Change*; Springer: Berlin/Heidelberg, Germany, 2014; pp. 249–264.
49. Lopez, M.G.; Di Baldassarre, G.; Seibert, J. Impact of Social Preparedness on Flood Early Warning Systems. *Water Resour. Res.* **2017**, *53*, 522–534. [CrossRef]
50. Pappenberger, F.; Cloke, H.L.; Parker, D.J.; Wetterhall, F.; Richardson, D.S.; Thielen, J. The Monetary Benefit of Early Flood Warnings in Europe. *Environ. Sci. Policy* **2015**, *51*, 278–291. [CrossRef]
51. Johnson, L.E.; Cifelli, R.; White, A. Benefits of an Advanced Quantitative Precipitation Information System. *J. Flood Risk Manag.* **2020**, *13*, e12573. [CrossRef]
52. ATTOM. ATTOM Data Solutions. Available online: https://www.attomdata.com/ (accessed on 1 January 2019).
53. US Census Bureau QuickFacts: Santa Clara County, California. Available online: https://www.census.gov/quickfacts/santaclaracountycalifornia (accessed on 1 January 2019).